2017 IEEE/RSJ International Conference on Intelligent Robots and Systems (IROS)
September 24–28, 2017, Vancouver, BC, Canada

A Leg Design Method for High Speed Quadrupedal Locomotion*

Spyridon Dallas, Konstantinos Machairas, Konstantinos Koutsoukis, *Student Members, IEEE*, and Evangelos Papadopoulos, *Senior Member, IEEE*

Abstract— **This paper introduces a leg design method aiming at speed maximization for quadruped robots with two-segment compliant legs, in trotting and bounding. The proposed method is an effort to address the leg design challenge in a holistic way, exploiting the coupling between gait parameters, leg design parameters and hardware constraints, while remaining control scheme independent. Optimal body trajectories and footfalls are derived using a simplified centroidal dynamics model, whereas joint trajectories and torques are computed by a more complex dynamic model, incorporating actuation parameters and constraints. The method is applied using real robot parameters to yield an optimal leg design, validated through a realistic trotting simulation experiment. In this experiment, the robot achieves accelerating motion from stance towards the maximum speed predicted by the method.**

I. Introduction

Recently, research in the field of unmanned terrestrial locomotion has focused in the advantages offered by legged robots. Quadruped robots seem promising in traversing uneven or rugged terrain in comparison to wheeled or tracked systems. As the legs are the means of interaction with the ground, the robot performance strongly depends on leg design. Critical design choices include the number of the leg segments, the segment proportions, the configuration of the mechanism (e.g. forward vs backward pointing knee), and the stiffness of any passive compliant elements. For deciding upon such matters, various approaches have been adopted.

Many research teams have been inspired from biological data. For instance, the length and proportions of the Cheetah Cub's legs were taken similar to these of small felids [1]. The leg length of the HyQ robot was chosen based on observations made by dog and horse breeders [2]. The leg proportions of the Pneupard robot were based on anatomical data of the Cheetah [3]. However, even though the musculoskeletal system of animals has gone through nature's optimization process, robotic tasks and actuation significantly differ from the animals' survival tasks and muscle actuation.

Other researchers have based their design approach on simplified dynamics, where the leg is studied decoupled from the body for simplicity. The effect of joint configuration and angle of attack were studied for two-segment legs based on energy losses due to collisions with the ground [4]. Another approach focused on the kinematics of legged locomotion and sought the optimal leg based on manipulability measures [5]. The role of the shoulder's height, the touchdown configuration and the range of motion for producing the desired supportive body forces for running were studied for the leg of the MIT Cheetah [6]. The stiffness of the compliant elements of StarlETH's legs was selected to minimize actuator work in a model of a single-legged hopper [7].

Finally, some approaches are based on full quadruped robot models. The role of knee configuration in pitching moments was studied for a trotting quadruped [8]. The study included legs with fixed proportions, inertial properties and stiffness for a specified control scheme. The role of leg stiffness, leg length and touchdown angle, in the energetic cost of transport of a bounding robot were studied in [9]. The model used however was applicable only for prismatic legs with no inertia. Optimal trajectories were produced for different tasks with a centroidal dynamics approach and leg proportions were found that minimized the squared sum of joint torques [10]. The leg configuration however was predetermined, passive elements were absent from the dynamics, and motor and strength of material constraints were not taken into account. For a bounding robot model with fixed leg proportions and configuration, the stiffness of compliant passive elements was found that minimizes power consumption at a given running speed [11].

In this work, we introduce a leg design method for quadruped robots with two-segment compliant legs, aiming in locomotion speed maximization. This method is an effort to address the problem of leg design holistically, exploiting the relation between gait parameters (gait, stride period, ground reaction forces), leg design parameters (leg length, proportioning, stiffness and joint configuration) and hardware constraints (leg material and spring properties, motor and gearhead operating ranges). Centroidal dynamics are used to facilitate trajectory optimization and more complex dynamics for the accurate calculation of the motor requirements. The method is applied with the parameters of an actual robot, and the optimal attributes are found that maximize speed while respecting hardware constraints. The optimal results are validated in a realistic simulation scenario, involving energy losses, a ground model, and acceleration from stance towards the highest forward velocity predicted by the method.

The structure of the paper is as follows. In Section II, the method elements (gaits, dynamics, and joint trajectories calculation) are presented. Section III discusses in detail the method framework and the connections between its building elements. The method is applied using real robot parameters and its results are presented in Sections IV and validated in Section V. Section VI concludes the paper.

II. Elements of the Method

The developed method inputs include the robot body inertial parameters, the hardware constraints and the gait performed, and finds the optimal leg design and the gait parameters under which the highest forward speed can be reached. To this end, the method initially uses simplified sagittal centroidal dynamics to find the optimal body CoM trajectory and leg footfalls for a specified gait. Using these

*This research has been financed by the "IKY Fellowships of Excellence for Postgraduate Studies in Greece – Siemens Programme" in the framework of the Hellenic Republic – Siemens Settlement Agreement.

The authors are with the School of Mechanical Engineering, National Technical University of Athens, (e-mail: egpapado@central.ntua.gr, tel: +30 210-772-1440).

and the inverse kinematics and dynamics of a complex sagittal quadruped model, the trajectories and torques of the leg joints are derived, and hardware constraints are evaluated. The optimal design is a result of an iterative process consisting of the aforementioned steps. This section presents the necessary physical descriptions and calculations, which are used as building elements for the method.

A. *Gait description*

Among the various gaits used for quadrupedal locomotion [12], trotting and bounding gaits are employed by the vast majority of robots running in moderate and high velocities due to the symmetry and the small rolling motion they introduce (Fig. 1), allowing use of 2D sagittal plane models. The proposed method aiming at leg design for high-speed robots, subjected to current technological limitations, focuses on these gaits in particular.

In the developed method, the gait is determined by providing as inputs the touchdown and take-off time instants of the i-th leg, $t_{td,i}$ and $t_{to,i}$, where $i \in \{HL, FL, FR, HR\}$ corresponding to hind left, front left, front right and hind right leg respectively. Under the assumption of equal stance phase duration δt_s for all legs (Fig. 1), the duty factor of a leg in one stride period T is defined as:

$$DF = (t_{to,i} - t_{td,i}) / T = \delta t_s / T \tag{1}$$

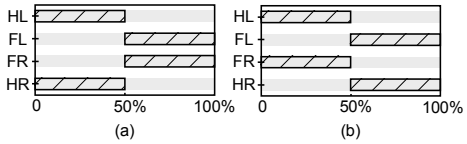

Figure 1. Gait graphs of (a) bounding gait (b) trotting gait.

B. *Quadruped dynamics*

To study the effect of leg design on quadrupedal locomotion, a sagittal model consisting of the main body and four identical legs is introduced. The main body of the quadruped model has mass m_b, inertia I_b and hip half separation distance d, see Fig. 2. Each leg has two actuated rotary joints and a passively compliant prismatic joint. The leg segments are considered tubular with outer diameter d_o, inner diameter d_i, density ρ and material strength S. For each leg, the proximal to the body leg segment has length l_1, mass m_1 and inertia I_1. The distal to the body compliant leg segment has free length l_{20}, mass m_2, inertia I_2, and spring stiffness k. The spring mass and inertia is lumped in the mass m_2 and inertia I_2 of the distal segment.

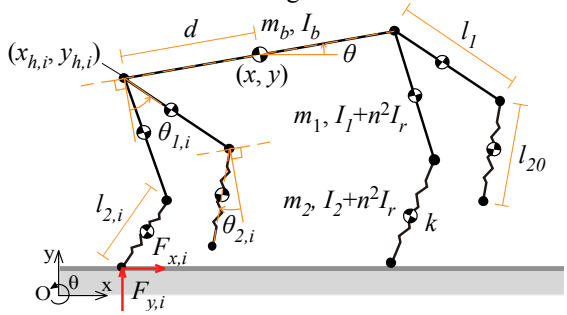

Figure 2. Quadruped robot model.

The actuators are modeled as DC motors with gear ratio n and rotor inertia I_r, and they are mounted on the body for lighter legs. The thermal limits of the motor and the mechanical limits of the gearbox, define maximum values for the short-term torque $\tau_{st,max}$, the continuous torque $\tau_{ct,max}$ and the angular velocity $\dot{\theta}_{\max}$.

The system is described in terms of the generalized coordinate vector $\mathbf{q}$, which consists of the body Center of Mass (CoM) position (x, y), the body pitch angle θ, and the joint variables of each leg $\theta_{1,i}$, $\theta_{2,i}$, $l_{2,i}$. Each time the i-th leg contacts the ground, forces $F_{x,i}$ and $F_{y,i}$ are applied by the ground to the leg. Following the Euler - Lagrange formulation, the Equations of Motion (EoM) are written as:

$$\mathbf{M}\ddot{\mathbf{q}} + \mathbf{C}\dot{\mathbf{q}} + \mathbf{K}\mathbf{q} + \mathbf{J}^T\mathbf{F} = [\mathbf{0}\ \boldsymbol{\tau}]^T \tag{2}$$

where $\mathbf{M}$ is the mass matrix, $\mathbf{C}$ the centrifugal/Coriolis terms matrix, $\mathbf{K}$ is the stiffness matrix, $\mathbf{J}$ is the Jacobian matrix of the legs and $\boldsymbol{\tau}$ is a vector consisting of the torques $\tau_{j,i}$, acting on every actuated joint ($j=1, 2$) of every leg.

C. *Simplified centroidal dynamics*

With the centroidal dynamics approach, the dynamics of the system are projected to its CoM. This approach has been used for CoM trajectory optimization [10], [13] and postural balance control of legged robots [14]. The legs of quadruped robots are lightweight and therefore changes in leg posture do not significantly affect the position of the CoM. With this assumption the centroidal dynamics are simplified, yielding:

$$\ddot{x} = F_x / m \tag{3}$$

$$\ddot{y} = F_y / m - g \tag{4}$$

$$\ddot{\theta} = \tau_\theta / \mathrm{I} \tag{5}$$

where g is the gravitational acceleration, and m, and I are the mass and inertia of the centroidal model given by

$$m = m_b + 4(m_1 + m_2),\ I \simeq I_b \tag{6}$$

F_x, F_y, are the forces and τ_θ is the torque acting on the CoM,

$$F_x = \sum_i c_i F_{x,i} \tag{7}$$

$$F_y = \sum_i c_i F_{y,i} \tag{8}$$

$$\tau_\theta = \sum_i c_i \mathbf{r}_i \times \mathbf{F}_i \cdot \hat{\mathbf{z}} = \sum_i c_i \left[(x_i - x)F_{y,i} - (y_i - y)F_{x,i} \right] \tag{9}$$

where c_i is equal to 1 when the i-th leg is in contact with the ground and 0 otherwise, $\mathbf{r}_i$ is the vector connecting the CoM position (x, y) with the footfall of the i-th leg (x_i, y_i), $\mathbf{F}_i$ is the vector of the horizontal and vertical forces $F_{x,i}$, $F_{y,i}$ exerted on the i-th toe and y_i=0 with the assumption that locomotion takes places on even terrain, see Fig. 3.

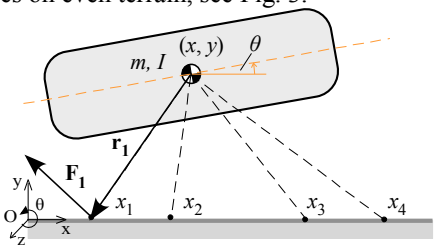

Figure 3. Centroidal dynamics model and its properties.

Observing simulation results of leg models, [15], experimental data from running quadruped animals [16]-[17], and from quadruped robots [1], [18], [19], the vertical ground force has a profile close to a half-sine impulse, while the horizontal force resembles a decelerating - accelerating

sinusoidal profile. Therefore, here the forces $F_{y,i}$, $F_{x,i}$ exerted on the i-th toe are described as sinusoidal functions with their arguments lying in [0, π], and in [π, 3π] respectively:

$$F_{y,i}(t) = F_{y,\max} \sin(\omega_y t + \varphi_{y,i}) \quad (10)$$

$$F_{x,i}(t) = F_{x,\max} \sin(\omega_x t + \varphi_{x,i}) \quad (11)$$

By applying boundary conditions to the arguments of $F_{x,i}$, and $F_{y,i}$, the $\omega_{x,i}$, $\varphi_{x,i}$, $\omega_{y,i}$, $\varphi_{y,i}$ are found as functions of the $t_{td,i}$, $t_{to,i}$, δt_s, and given by,

$$\omega_y = \pi / \delta t_s, \quad \varphi_{y,i} = -\pi t_{td,i} / \delta t_s \quad (12)$$

$$\omega_x = 2\pi / \delta t_s, \quad \varphi_{x,i} = \pi(t_{to,i} - 3t_{td,i}) / \delta t_s \quad (13)$$

Employing the classic Coulomb friction model, for a leg to remain in contact with the ground without slipping, (14) must hold, where μ is the Coulomb friction coefficient. Thus an upper bound (subscript *ub*) is set for the horizontal force amplitude in (15) so that (14) is valid throughout the stride.

$$\left|F_{x,i}(t)\right| \le \mu F_{y,i}(t) \quad (14)$$

$$F_{x,\max} \le F_{x,ub} \quad (15)$$

Introducing a_{fx}, inequality (15) is expressed as an equation,

$$F_{x,\max} = a_{fx} F_{x,ub}, \ a_{fx} \in [0,1] \quad (16)$$

To move *periodically* in the y and θ directions with a steady net forward velocity in the x direction, the robot should not have any net acceleration in any direction in a single stride circle, and thus (17), (18) and (19) must hold:

$$\int_0^T F_x dt = 0 \quad (17)$$

$$\int_0^T F_y dt = mgT \quad (18)$$

$$\int_0^T \tau_\theta dt = 0 \quad (19)$$

Note that the horizontal force profile defined in (11) already satisfies (17). From (18) and taking into account (1), (8) and (12), the amplitude of $F_{y,I}$ is written as:

$$F_{y,\max} = \frac{mgT\omega_y}{8} = \frac{\pi mgT}{8\delta t_s} = \frac{\pi mg}{8DF} \quad (20)$$

D. Leg joint trajectories

While the centroidal dynamics approach focuses on the CoM motion, if the robot's geometry is known, motion in joint space can be found using the inverse kinematics of the sagittal model of the quadruped shown in Fig. 2,

$$\theta_{1,i} = f(x, y, \theta, d, l_1, l_{2,i}, x_{t,i}, y_{t,i}) \quad (21)$$

$$\theta_{2,i} = g(x, y, \theta, d, l_1, l_{2,i}, x_{t,i}, y_{t,i}) \quad (22)$$

where ($x_{t,i}$, $y_{t,i}$) are the toe coordinates. Note that for the case of two-segment legs, two alternative sets are obtained from (21) and (22), corresponding either to a knee backward or a knee forward configuration.

During stance phase, if (14) holds, the legs remain in contact with the ground,

$$(x_{t,i}, y_{t,i}) \equiv (x_i, 0), \ t \in [t_{td,i}, t_{to,i}] \quad (23)$$

The geometry of the leg changes during the stance phase due to spring compression. Therefore, apart from the inverse kinematics equations, also an equation referring to the spring compression must be introduced. By projecting the ground forces in the direction of the spring (compressive force is negative by consensus), the spring force is,

$$F_{s,i} = F_{x,i} \sin(\theta + \theta_{2,i}) - F_{y,i} \cos(\theta + \theta_{2,i}) \quad (24)$$

From the definition of an ideal spring with no pretention,

$$F_{s,i} = k(l_{2,i} - l_{20}) \quad (25)$$

Using (24) and (25), the compliant leg segment deflection is obtained as a function of the ground forces and posture,

$$l_{2,i} = l_{20} + [F_{x,i} \sin(\theta + \theta_{2,i}) - F_{y,i} \cos(\theta + \theta_{2,i})] / k \quad (26)$$

Through (21), (22), and (26), the leg joint variables $\theta_{1,i}$, $\theta_{2,i}$, $l_{2,i}$ can be written as functions of the centroidal variables during stance phase. By differentiating (21), (22), and (26), the rates of the joint variables $\dot{\theta}_{1,i}, \dot{\theta}_{2,i}, \dot{l}_{2,i}$ are found, too.

In flight phase, the spring length is constant, equal to its free length, ($l_{2,i}$=l_{20}). The requirement for each leg during flight phase is to avoid collision with the ground by creating the necessary toe-to-ground clearance, following a first order continuous trajectory; non-continuous angular velocities would require infinite torques. Inspired by control schemes in which the reference toe trajectory during flight is an ellipse [20], a hybrid cubic polynomial/elliptical flight phase trajectory is selected. The cubic polynomial part ensures continuity for angular velocities, and the elliptical part provides realistic boundary conditions at midflight. The cubic polynomials used to interpolate the angular positions from take-off to mid-flight (subscript *mf*) and from mid-flight to touchdown are of the form,

$$\theta_{j,i,n} = \alpha_{j,i,n} t^3 + \beta_{j,i,n} t^2 + \gamma_{j,i,n} t + \delta_{j,i,n} \quad (27)$$

where j=1, 2 correspond to the hip and knee joints and n=1, 2 correspond to $t \in [t_{to,i}, t_{mf,i}]$ or $t \in [t_{mf,i}, t_{td,i}]$. Differentiating (27), the angular velocities are obtained as,

$$\dot{\theta}_{j,i,n} = 3\alpha_{j,i,n} t^2 + 2\beta_{j,i,n} t + \gamma_{j,i,n} \quad (28)$$

The state of the leg at take-off and touchdown can be found from the preceding stance phase. Therefore, to find the coefficients of the cubic polynomials, only the state of the leg at midflight is needed, here taken at the apex of an ellipse,

$$(x_{t,i}, y_{t,i}) \equiv (x_i + a_e, b_e) \quad (29)$$

$$(\dot{x}_{t,i}, \dot{y}_{t,i}) \equiv (\omega_e a_e, 0) \quad (30)$$

where a_e is the horizontal semi-axis of the ellipse,

$$a_e = [x(T) - x(0)] / 2 \quad (31)$$

b_e is the vertical semi-axis equal to desired clearance from the ground, and ω_e is the frequency of traversing the ellipse,

$$\omega_e = 2\pi / \mathrm{T}_e = \pi / [T(1 - DF)] \quad (32)$$

Using (29), (30), inverse kinematics and differential inverse kinematics, the joint angles and angular velocities are found at midflight. Finally, the coefficients of the cubic polynomials are found, by applying boundary conditions at take-off, midflight and touchdown in (27), (28).

III. Method Development

Given a robot's actuation system parameters and its mass/inertia properties, the developed method provides optimal leg parameters for achieving the maximum velocity in trotting and bounding gaits. The method consists of an outer stage and of two inner ones, as shown in Fig. 4. In the *outer stage*, the entire gait parameter space is spanned in terms of stride period, CoM height, CoM forward velocity, and horizontal ground force profile. For each gait parameter set, the *first inner stage* searches for the optimal CoM trajectory and the optimal footfalls using the simplified centroidal model. The goal of this optimization procedure is

to identify a periodical stride, while minimizing the torques necessary to sustain vertical ground forces.

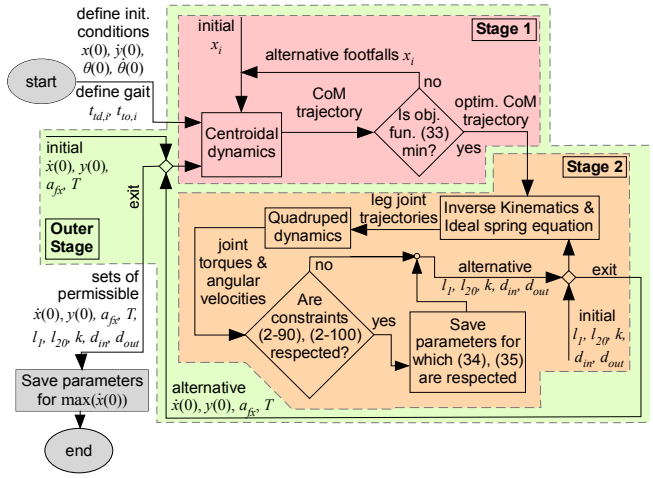

Figure 4. Flow chart indicating the different stages of the method.

In the *second inner stage*, the leg design parameters, including segment lengths and spring stiffness, are sought for the optimized CoM trajectory, so that the toe remains in the workspace of the leg, undesired collisions of the robot with the ground are avoided, and strength and actuation constraints are respected. As the desired forward velocity increases, the number of successful leg designs is expected to decrease. The optimal design parameters set is the one for which the robot achieves the maximum forward velocity. The stages are described in more detail next.

A. Outer Stage: Spanning the gait parameter space

The same two stage procedure is repeated for alternative gait related parameters T, $y(0)$, a_{fx} and with an increasing forward velocity $\dot{x}(0)$. The procedure conducted in the outer stage is an exhaustive search, i.e. a search of optimal parameters in 'for' loops. The target of this exhaustive search is to maximize the horizontal velocity $\dot{x}(0)$. The method exits when the maximum $\dot{x}(0)$ is reached where a stable stride with reduced hip joint torques can be found (Stage 1) and strength/actuation constraints are valid (Stage 2).

B. Inner Stage 1: CoM trajectory & footfall optimization

The first inner stage has as inputs the initial conditions for the motion of the centroidal model $x(0)$, $\dot{x}(0)$, $y(0)$, $\dot{y}(0)$, $\theta(0)$, $\dot{\theta}(0)$, the gait period T, the time instants of touchdown and take-off as a percentage of the period for each leg, $t_{td,i}$, $t_{to,i}$ and the magnitude of the horizontal force a_{fx}. The abscissas of the footfalls x_i are sought for minimizing the weighted sum,

$$Q = w_1\left|\theta(\mathrm{T})-\theta(0)\right| + w_2\left|\dot{\theta}(\mathrm{T})-\dot{\theta}(0)\right| + w_3\sum_i\int_{t_{td,i}}^{t_{to,i}}\left|x_{h,i}-x_i\right|dt \quad (33)$$

where $x_{h,i}$ is the abscissa of the hip joint, see Fig. 2. The first two terms ensure that the motion in the θ direction is periodic in one stride. By minimizing these terms, no net acceleration in the θ direction exists, so (19) is satisfied. The third term ensures that the footfall abscissa of the i-th leg stays in the vicinity of the hip joint abscissa during the stance phase, thus minimizing the moment arm from the hip joint. As a result, the torques required to sustain vertical forces are minimized.

In each optimization loop, alternative x_i are inserted as inputs, (3)-(5) are solved numerically for one stride as an initial value problem (IVP), the body is checked not to collide with the ground, and the objective function is evaluated. The IVP is solved with a fixed step third order Runge-Kutta solver (MATLAB `ode3`), for N=1000 points, achieving thus high result accuracy and solution speed. The optimization consists of an exhaustive search step, followed by an interior point optimization step (MATLAB `fmincon`). The exhaustive search step locates crudely the area of the optimum point without getting trapped in local optima. Then the interior point algorithm is applied in this parameter area and locates the optimum point with fine accuracy. The outputs of this stage include the optimal footfall abscissas $x_{i,o}$, the vector of the discrete integration time $\boldsymbol{t}$ and the vectors of the optimal CoM trajectory, $\mathbf{q}_C = [x\, y\, \theta]$, $\dot{\mathbf{q}}_C$, $\ddot{\mathbf{q}}_C$.

C. Inner Stage 2: Spanning the leg parameter space

In the second inner stage, with the trajectory of the CoM available at discrete time instants, the inverse kinematics are solved for alternative leg parameters l_1, l_{20} and k, (see Section II, Par. D) for a preferred knee configuration, and the vectors of joint variables $\mathbf{q}_{jnt,i} = [\theta_{1,i}\ \theta_{2,i}\ l_{2,i}]$ are found. The knee joints are checked not to collide with the ground. For the leg posture, and the ground forces exerted on the toe at every time instant, optimal diameters d_{in}, d_{out} are sought satisfying the strength constraints,

$$\sigma_{j,i} \le S / s_f \quad (34)$$

where $\sigma_{j,i}$ is the stress on the cross-sectional area of every tubular segment (j=1, 2) of a leg, and s_f is a user defined safety factor. By numerically differentiating the vectors of joint positions, the first and second order derivatives $\dot{\mathbf{q}}_{jnt,i}$, $\ddot{\mathbf{q}}_{jnt,i}$ are calculated using central difference expressions (`gradient`, `del2`). By replacing the values of $\mathbf{q}_C$, $\mathbf{q}_{jnt,i}$ and their derivatives in (2), the actuation torques $\boldsymbol{\tau}$ are calculated. The vectors of torque and angular velocity of every actuated joint (j=1, 2) of all legs are subject to actuation constraints,

$$\max_t(\tau_{j,i}) \le \tau_{st,\max},\ \ \mathrm{rms}_t(\tau_{j,i}) \le \tau_{ct,\max},\ \ \max_t(\dot{\theta}_{j,i}) \le \dot{\theta}_{\max} \quad (35)$$

where rms(.) finds the rms value over time. If constraints (34), (35) are satisfied then the gait related parameters $\dot{x}(0)$, $y(0)$, T, a_{fx}, and leg parameters l_1, l_{20}, k, d_{in}, d_{out} are saved.

The outer stage chooses the optimal set of gait and leg-related parameters as the one for which the quadruped robot can run stably in maximum forward velocity $\dot{x}(0)$, respecting the constraints.

IV. Method Application Results

The developed method was applied for the bounding and the trotting gaits, both for the knee backward (KB) and the knee forward (KF) configurations. The robot parameters were taken similar to those of the quadruped robot Laelaps of NTUA [21], see Table I. The times of touchdown and take-off for each leg for the bounding and the trotting gaits were taken as shown in Fig. 1 (a), (b), as a percentage of the stride period, assuming running with a constant leg duty factor DF=0.5. In future versions of the developed method, the DF will be included in the parameters to be optimized, but for the results presented here, it is kept constant. Initial conditions

not optimized are user defined, taken as $x(0)$=1 m, $\dot{y}(0)$ =0 m/s, $\theta(0)$=0 rad. The initial pitching rate of the trotting gait is set to $\dot{\theta}(0)$ =0 rad/s and that of the bounding gait to

$$\dot{\theta}(0)_{bound} = \theta_{\max} 2\pi / \mathrm{T} \tag{36}$$

where $\theta_{\max}$=10π/180 rad is the maximum accepted pitch angle. Parameters l_1, l_{20} were sought using a third one, ε,

$$l_1 \in [0.1, \varepsilon l_{\max} - 0.1],\ l_{20} = \varepsilon l_{\max} - l_1 \tag{37}$$

where $\varepsilon \in [1,1.1]$ and l_{max} is the maximum hip to toe distance for any leg during one stride,

$$l_{\max} = \max_{i,t} \sqrt{(x_{t,i} - x_{h,i})^2 + (y_{t,i} - y_{h,i})^2} \tag{38}$$

The lower and upper bounds (lb, ub) for the remaining parameters were set as shown in Table II, so that in maximum velocity, optimal solutions would not be truncated by them. The weights (w_1, w_2) of (33) were taken equal to (10, 1) to ensure the first two terms have the same magnitude. The third weight was selected to be w_3=1 to achieve torque reduction without jeopardizing stability.

TABLE I. VALUES OF ROBOT PARAMETERS.

Parameter	Value	Parameter	Value
m (kg)	42.0	S (MPa)	200.00
d (m)	0.30	s_f	3.00
I (kg·m^2)	3.58	n	53.00
μ	0.65	I_r (kg m^{2}10^{-5})	5.42
g (m/s^2)	9.81	$\tau_{st,max}$ (Nm)	45.00
b_{tr} (m)	0.05	$\tau_{ct,max}$ (Nm)	14.96
ρ (kg/m^{3}10^2)	14.66	$\dot{\theta}_{\max}$ (rad/s)	11.21

TABLE II. UPPER AND LOWER BOUNDS OF PARAMETER SPACE.

Parameters & Initial Condition	Bounding		Trotting	
	LB	UB	LB	UB
$y(0)$ (m)	0.45	0.85	0.55	1.30
k (N/m)	1250	5000	1250	7500
T (s)	0.20	0.60	0.35	0.75
a_{fx}	0	0.6	0.1	0.7
d_i, (mm)	20	28	20	28
d_o (mm)	22	30	22	30

For trotting with increasing horizontal velocity, the combinations of parameters for which constraints (34), (35) were valid decreased until convergence at maximum speed, see Fig. 5. The trajectories of the centroidal model at maximum forward velocity are also presented (Fig. 6) as proof of concept that (33) yields a periodical stride. Similar results were also encountered for bounding. For the trotting gait, the maximum velocity reached was 2.900 m/s for the KB configuration, and 2.940 m/s for the KF configuration. For the bounding gait, the maximum forward velocity was 0.479 m/s for the KB configuration, and 0.540 m/s for the KF configuration. For both gaits, the KF configuration had only a slight advantage over the KB configuration. The trotting gait was shown to be much faster than the bounding gait. Probably this is due to the excessive pitching of the latter, which leads the legs to support the robot weight during stance phase in an unfavorable crouched posture, resulting in greater torque requirement for lower forward velocity. The parameters for which these maximum velocities were achieved are displayed in Table III. The corresponding leg architectures are depicted in Fig. 7. The insufficiency of actuating torques for the bounding gait led to small leg segments, see Fig. 7 (a). In the case of the trotting gait, an interesting tall leg architecture resulted, with a short upper and a long lower segment with a soft spring, Fig. 7(b). Long legs enhance running velocity by increasing the stride length. With these legs, during stance most of the leg deflection is undertaken by the passive element, allowing the robot to withstand ground forces in a near singular configuration. During flight phase, the hip motor acts on the entire leg (of length l_1+l_{20}) whereas the knee motor acts on the segment with length l_{20}. The optimal l_1 derived from the proposed method is significantly smaller than l_{20}, so that the load of the swinging task is in a way distributed to both leg motors. Nevertheless, a long leg approach leads to a top-heavy robot, perhaps vulnerable to instabilities due to external perturbations, a factor that is not taken into account by the current version of the method. Intrigued by the opportunities/risks trade-off a long leg of this architecture could offer for the trotting gait, we decided to further evaluate the leg with a simulation independent to the method.

TABLE III. OPTIMAL PARAMETERS IN MAXIMUM VELOCITIES.

Gait/ Config.	$y(0)$ (m)	T (s)	a_{fx}	l_1 (m)	l_{20} (m)	k (N/m)	d_{in} (mm)	d_{out} (mm)
Bound/KB	0.55	0.30	0.1	0.36	0.23	3750	26	28
Bound/KF	0.50	0.30	0.1	0.30	0.24	3750	26	28
Trot/KB	1.20	0.60	0.4	0.20	1.10	2500	23	25
Trot/KF	1.25	0.60	0.4	0.20	1.16	2500	23	25

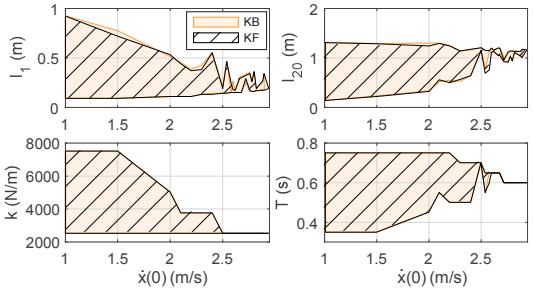

Figure 5. Evolution of parameters with forward trotting velocity for the knee backward (KB) and the knee forward (KF) configurations.

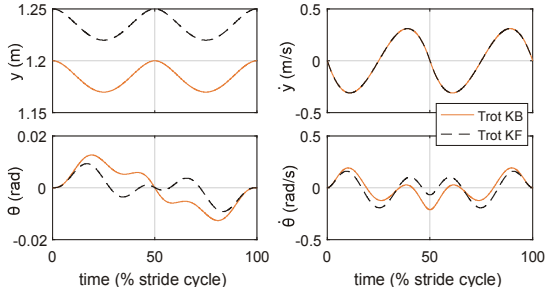

Figure 6. CoM trajectories for optimal parameters in trotting.

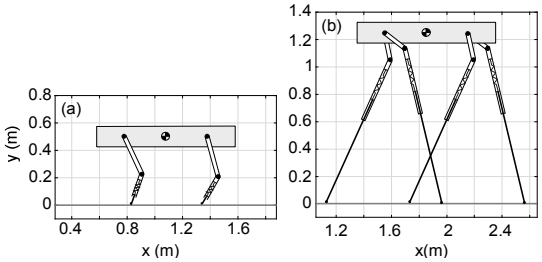

Figure 7. Optimal legs for the (a) bounding and the (b) trotting gait.

V. Validation of Method Results

To validate methods such as the developed one, evaluation tests are required to show that the planned tasks can be practically performed by the optimized designs, and that the assumptions made in all stages are reasonable. The simulation environment and the controller presented in [20] were used here to simulate a realistic trotting scenario including acceleration from stance to the highest forward velocity predicted by the method (2.94 m/s) for a 2D quadruped with two-segment knee-forward compliant legs. The model parameters were those of the robot Laelaps, see Table I, and the leg design and gait parameters were set to the optimal values given in Table III. Energy losses at all joints and a compliant ground model were included, and actuation constraints were taken into account – the joint torques and speed limits were set to 45 Nm and 11.21 rad/s respectively. The results are depicted in Fig. 8.

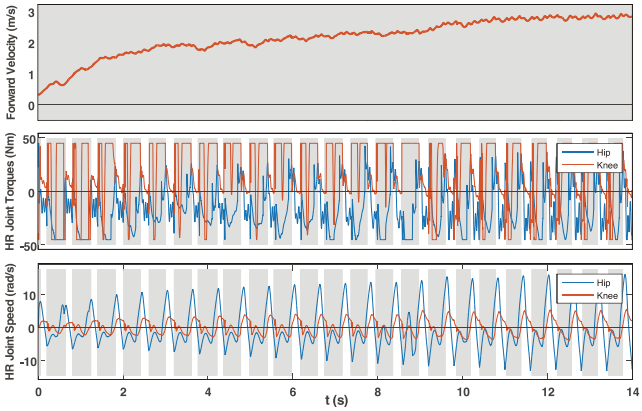

Figure 8. Simulation results from a trotting experiment, showing from top to bottom: the body's forward velocity from stance to maximum speed, and the torques and speeds at HR joints. The stance phase of each leg is denoted with gray backround color.

The results show that the robot is capable of accelerating to the predicted forward velocity by gradually increasing the stride length towards the maximum permitted value, see Fig. 8, providing a first validation of the method. Yet, a couple of points concerning the torque-speed limits must be addressed. In Fig. 8 we observe that the maximum hip angular velocity exceeded the limit of 11.21 rad/s when running faster than 2m/s. This was due to leg motion at flight phases – white areas in Fig. 8; the toes were lifted higher than needed in every stride to increase the robustness of the gait, and this induced the high joint speeds. This mismatch is considered insignificant, since control modifications can be applied to achieve less clearance from the ground, and thus acceptable joint velocities. Secondly, we note that the body runs at lower height for stability reasons, meaning that the knees were more crouched than the method suggested, thus requiring higher than the predicted torques. It is evident that in this case also, modifications in the controller can yield results closer to those predicted by the method, with lower rms torques than those shown in Fig. 8. However, an overall increase in torque requirements should be expected due to energy losses at the joints, collisions with the ground, and also the accelerating nature of the task; these features were not considered in the method.

VI. Conclusion

In this paper a method was proposed for designing legs for running quadrupeds. Employing centroidal dynamics for CoM trajectory optimization, and quadruped dynamics and kinematics for actuation requirements estimation, optimal gait and leg design parameters were found for running in maximum speed with various gaits (bound, trot) and joint configurations (knee backward, knee forward). The long leg architecture that led to the overall maximum forward speed for the trotting gait was subjected to further evaluation using an independent robot simulation. The results showed good match of the performance predicted by the method to that provided by the independent simulation, demonstrating the validity of the developed method.

References

[1] A. Sprowitz et al., "Towards dynamic trot gait locomotion: Design, control, and experiments with Cheetah-cub, a compliant quadruped robot," *Int. J. of Robotics Research,* v. 32, no. 8, 2013, pp. 932-950.

[2] C. Semini, "HyQ - Design and Development of a Hydraulically Actuated Quadruped Robot," *Ph.D. dissertation*, University of Genoa & Italian Instute of Technology, 2010.

[3] S. Nakatsu et al., "Realization of Three-dimensional Walking of a Cheetah-modeled Bio-inspired Quadruped Robot," in *IEEE Int. Conf. on Robotics & Biomimetics*, Bali, Indonesia, 2014.

[4] M. Jones and J. Hurst, "Effects of leg configuration on running and walking robots," in *Int. Conf. on Climbing & Walking Robots (CLAWAR)*, Baltimore, 2012.

[5] G. Kenneally et al., "Design Principles for a Family of Direct-Drive Legged Robots," *IEEE Robotics & Automation Letters,* v. 1, n. 2, 2016, pp. 900-907.

[6] J. E. McKenzie, "Design of Robotic Quadruped Legs," *M.S. Thesis*, Massachusetts Inst. of Technology, 2012.

[7] M. Hutter, "StarlETH & Co. – Design and Control of Legged Robots with Compliant Actuation," *Ph.D. dissertation*, ETH Zurich, 2013.

[8] D. V. Lee and S. G. Meek, "Directionally compliant legs influence the intrinsic pitch behavior of a trotting quadruped," *Proc. of the Roy. Soc. B: Biological Sci.,* v. 272, no. 1563, 2005, pp. 567-572.

[9] P. Chatzakos and E. Papadopoulos, "Bio-inspired design of electrically-driven bounding quadrupeds," *Mechanism & Mach. Theory,* v. 44, 2009, pp. 559–579.

[10] S. Ha et al., "Task-based Limb Optimization for Legged Robots," in *IEEE/RSJ Int. Conf. on Intell. Robots & Syst. (IROS)*, Daejeon, 2016.

[11] G. Folkertsma et. al, "Parallel stiffness in a bounding quadruped with flexible spine," in *IEEE/RSJ Int. Conf. on Intell. Robots & Syst.*, Vilamoura, Algarve, Portugal, 2012.

[12] J. J. Collins and I. N. Stewart, "Coupled Nonlinear Oscillators and the Symmetries of Animal Gait," *J. of Nonlinear Sci.*, 1993, pp. 349-392.

[13] H. Dai et. al, "Whole-body motion planning with centroidal dynamics and full kinematics," in *IEEE-RAS Int. Conf. on Hum. Robots* , 2014.

[14] D. E. Orin et. al, "Centroidal dynamics of a humanoid robot," *Autononomous Robots,* v. 35, 2013, pp. 161-176.

[15] T. McMahon and G. Cheng, "The Mechanics of Running: How does stiffness couple with speed," *J. Biomech.,* v. 23, n. 1, 1990, pp. 65-78.

[16] R. M. Walter and D. R. Carrier, "Ground forces applied by galloping dogs," *The J. of Experimental Biology,* v. 210, 2007, pp. 208-216.

[17] P. E. Hudson et. al, "High speed galloping in the cheetah (Acinonyx jubatus) and the racing greyhound (Canis familiaris): spatio-temporal and kinetic characteristics," *J. Exp. Biol.,* v. 215, 2012, pp. 2425-2434.

[18] A. Ananthanarayanan et. al, "Towards a bio-inspired leg design for high-speed running," *Bioinspiration & Biomimetics,* v. 7, 2012.

[19] S. Seok et al., "Actuator Design for High Force Proprioceptive Control in Fast Legged Locomotion," in *IEEE/RSJ Int. Conf. on Intell. Robots & Syst.*, Vilamoura, Algarve, Portugal, 2012.

[20] K. Machairas and E. Papadopoulos, "An Active Compliance Controller for Quadruped Trotting," in *24th Mediterranean Conf. on Control & Automation (MED)*, Athens, 2016.

[21] https://nereus.mech.ntua.gr/legged